

Assessing the carbon and climate benefit of restoring degraded agricultural peat soils to managed wetlands

Kyle S. Hemes^{a,*}, Samuel D. Chamberlain^a, Elke Eichelmann^a, Tyler Anthony^a, Amy Valach^a, Kuno Kasak^{a,b}, Daphne Szutu^a, Joe Verfaillie^a, Whendee L. Silver^a, Dennis D. Baldocchi^a

^a Ecosystem Science Division, Department of Environmental Science, Policy and Management, University of California at Berkeley, USA

^b Department of Geography, Institute of Ecology and Earth Sciences, University of Tartu, Estonia

ARTICLE INFO

Keywords:

Greenhouse gas
Peat soil
Wetland restoration
Methane
Carbon dioxide
Sequestration

ABSTRACT

Restoring degraded peat soils presents an attractive, but largely untested, climate change mitigation approach. Drained peat soils used for agriculture can be large greenhouse gas sources. By restoring subsided peat soils to managed, impounded wetlands, significant agricultural emissions are avoided, and soil carbon can be sequestered and protected. Here, we synthesize 36 site-years of continuous carbon dioxide and methane flux data from a mesonetwork of eddy covariance towers in the Sacramento-San Joaquin Delta in California, USA to compute carbon and greenhouse gas budgets for drained agricultural land uses and compare these to restored deltaic wetlands. We found that restored wetlands effectively sequestered carbon and halted soil carbon loss associated with drained agricultural land uses. Depending on the age and disturbance regime of the restored wetland, many land use conversions from agriculture to restored wetland resulted in emission reductions over a 100-year timescale. With a simple model of radiative forcing and atmospheric lifetimes, we showed that restored wetlands do not begin to accrue greenhouse gas benefits until nearly a half century, and become net sinks from the atmosphere after a century. Due to substantial interannual variability and uncertainty about the multi-decadal successional trajectory of managed, restored wetlands, ongoing ecosystem flux measurements are critical for understanding the long-term impacts of wetland restoration for climate change mitigation.

1. Introduction

Working lands play an important role in terrestrial carbon (C) cycling, with the potential to be a source or a sink of carbon dioxide (CO₂) and other greenhouse gases (GHG) (Canadell and Schulze, 2014). Land management as a CO₂ removal strategy could remove up to 6 Gt CO₂ yr⁻¹ at a lower cost than more energy- and technology-intensive strategies (Psarras et al., 2017), with potential to help counteract society's growing soil C debt (Sanderman et al., 2017). The Intergovernmental Panel on Climate Change (IPCC) 5th assessment report stated that reversibility of anthropogenic climate change will only be possible with "large net removal of CO₂ from the atmosphere over a sustained period" (Myhre et al., 2013). Thus, C sequestration by ecosystems is of urgent importance, although limited by physical and ecological constraints (Baldocchi and Panuelas, 2018). Restoring degraded peat soils presents an attractive, but largely untested approach for soil C sequestration and associated climate change mitigation (Griscom et al., 2017; Leifeld and Menichetti, 2018; Paustian et al., 2016).

The benefits associated with wetland restoration for net C sequestration stem from two key areas. First, drained agricultural peat soils can be large GHG sources (Hatala et al., 2012; Knox et al., 2015; Schrier-Uijl et al., 2014; Veber et al., 2017). As organic-rich soils are drained and exposed to the atmosphere, aerobic respiration leads to large CO₂ emissions relative to flooded or saturated conditions that inhibit aerobic respiration. Globally, drainage of C-rich peat soils in river deltas has caused subsidence, the sinking of the land surface, as soil C is oxidized to CO₂ (Syvitski et al., 2009). This CO₂ source, along with emissions of other important agricultural GHG's like methane (CH₄) and nitrous oxide (N₂O), can cause agricultural peat soils to be large net emitters of GHGs. By restoring these subsided lands to managed, impounded wetlands, these agricultural emissions can be avoided. Second, the slow decomposition rates of wetland soil organic matter compared to high net primary productivity (NPP) leads to soil C accumulation. Maintaining wetland structure and function can protect much of the sequestered C and associated nitrogen from organic matter mineralization, leading to the potential for long-term C storage and

* Corresponding author at: Department of Environmental Science, Policy, and Management, University of California Berkeley, 130 Mulford Hall, Berkeley, CA 94720, USA.

E-mail address: khemes@berkeley.edu (K.S. Hemes).

<https://doi.org/10.1016/j.agrformet.2019.01.017>

Received 31 October 2018; Received in revised form 10 January 2019; Accepted 11 January 2019

0168-1923/ © 2019 Elsevier B.V. All rights reserved.

lower N₂O emissions (Deverel et al., 2016, 2014; Yarwood, 2018), although there is evidence that C sequestration capacity may not return to its pre-restoration rates (Moreno-Mateos et al., 2017, 2012).

Wetland restoration comes with a biogeochemical compromise, however (Hemes et al., 2018a; Hoper et al., 2008; Petrescu et al., 2015). While flooded wetland systems have the potential to sequester C as NPP outpaces soil respiration, the highly reduced conditions can result in significant CH₄ emissions (Bridgman et al., 2013; Dean et al., 2018), often making restored wetlands net GHG sources to the atmosphere over decadal timescales (Hemes et al., 2018a). Due to limited long-term continuous data in restored wetlands of various ages, many future climate scenarios have treated restored wetlands and peatlands as GHG neutral (Griscom et al., 2017; Leifeld and Menichetti, 2018). A recent rise in global atmospheric CH₄ concentrations has renewed interest in characterizing the contribution of wetlands to global biogeochemistry and radiative forcing, which is likely around 30% of all anthropogenic and natural CH₄ sources (Feldman et al., 2018; Nisbet et al., 2016; Poulter et al., 2017). Future projections of wetland CH₄ emissions suggest that they could play an important role in driving climate change throughout the 21st century (Dean et al., 2018; Zhang et al., 2017). Despite this fact, the balance between GHG emissions and C sequestration in wetlands remains an “enigma” (Mitsch and Mander, 2018). Long-term, in-situ, continuous measurements of GHG exchange over these ecosystems are critical to resolve their biogeochemical impact (Hemes et al., 2018a; Petrescu et al., 2015).

The Sacramento-San Joaquin River Delta is a hydrologically critical mosaic of drained and subsided agricultural peat soils that has been undergoing wetland restoration activities in order to reverse subsidence and accrete soil for up to two decades. This region provides a useful test of the climate impacts of ‘wet’ restoration on degraded peat soils. Delta GHG budgets have been published for a single growing season, demonstrating that over 2012–2013, a mature wetland was a GHG sink while a younger wetland was a net source of GHG (Knox et al., 2015). During another year at a single restored wetland site (West Pond) in the Delta, Windham-Myers et al. (2018) report GHG neutrality from combined chamber and eddy covariance measurements. Other studies of wetlands in the Delta have reported net GHG sources, and switchover times (from a source to a sink) of greater than 500 years (Anderson et al., 2016; McNicol et al., 2016).

Drained, subsided agricultural land uses in the Delta have also been individually investigated for GHG and water exchange. Multiyear measurements at a rice paddy (Twitchell Rice) tied large interannual variability in the net C budget to variability in ecosystem respiration (R_{eco}) driven by soil temperature (Knox et al., 2016). Teh et al. (2011) found an intermittently inundated pasture (Sherman pasture) in the Delta to be a large source of N₂O emissions ($2.4 \pm 1.3 \text{ g N}_2\text{O-N m}^{-2} \text{ yr}^{-1}$) and a modest source of CH₄ ($1.6 \pm 1.4 \text{ g CH}_4\text{-C m}^{-2} \text{ yr}^{-1}$ to $9.5 \pm 3.4 \text{ g CH}_4\text{-C m}^{-2} \text{ yr}^{-1}$) during 2007–2008. The same pasture was a modest GHG source over 2009–2010 (Hatala et al., 2012). Corn and alfalfa represent other dominant and water-intensive land uses in the Delta (Anderson et al., 2018; Eichelmann et al., 2018) that have important GHG implications. Concurrent observations of ecosystem-scale GHG exchange at both restored wetlands and drained agricultural peat soils in close proximity allows for a space-for-time assessment of the climatic effect of land use conversion.

Here, we synthesized 35 site-years of continuous CO₂ and CH₄ flux data from a mesonetwork of eddy covariance towers in the Delta to compute C and GHG budgets at agricultural sites with drained, degraded peat soils and a chronosequence of four freshwater deltaic restored wetlands. We also integrated N₂O chamber measurements from two of the agricultural sites. Our study sites represent a suite of dominant and potential future land uses in the Delta region, and differ climatically and ecologically from other studied restored wetlands and peatlands, many of which are in northern high-latitude climates. Our study aimed to address the hypothesis that land use change from agriculture on drained, degraded peat soils to freshwater, deltaic

restored wetlands, will result in a net GHG benefit over multi-decadal timescales, while accreting soil and sequestering C from the atmosphere into the ecosystem. Along with climate benefits, these ecosystem services have the potential to halt and reverse soil subsidence and protect the fragile hydrological network through which water is transported across California. Further, we assessed what specific land use transitions optimize GHG emission reductions, and quantified the impact of a set of global warming potential (GWP) metrics on this determination.

2. Materials & methods

2.1. Site characteristics

The Sacramento–San Joaquin River Delta was once a vast 1400 km² wetland and riparian zone fed by two of California’s largest rivers (Atwater et al., 1979; Cloern and Jassby, 2012). Since drainage in the mid-19th century (Weir, 1950) much of the land surface has been subsiding dramatically, losing close to 200 Tg C due to drainage-induced oxidation of the peat soils (Drexler et al., 2009). A series of dikes and levees protect the subsided ‘islands’ by holding back the rivers and sloughs that deliver at least a portion of the drinking water to more than two-thirds of Californians through the State Water Project and the Central Valley Project. Generally, wetland soils are highly organic while agricultural soils exhibit a mixed layer of degraded oxidized peat and mineral soil on top with a deep peat horizon below (Miller et al., 2008). Historically, mixed alluvium mollisols formed adjacent to major rivers, while organic histosols were found where fluvial deposition was less pronounced (Atwater et al., 1979; Chamberlain et al., 2018; Deverel and Leighton, 2010). The ten sites considered in this study, described in detail in Table S1, are located on Twitchell, Sherman, and Bouldin Islands, and are composed of four restored wetlands and six agricultural sites that make up most of the dominant land uses in the Delta region. Individual study sites have been described in previous work and will be summarized here for brevity (Chamberlain et al., 2018; Eichelmann et al., 2018; Hatala et al., 2012; Knox et al., 2015; Oikawa et al., 2016b). These sites are all part of the Ameriflux network (<http://ameriflux.lbl.gov/>) through which publicly available data and site information are available.

The Sherman wetland (Ameriflux ID: US-Sne; 263 ha) was restored from Sherman pasture in November of 2016 and was still in the process of establishing a fully vegetated canopy at the time of this study. East End restored wetland (US-Tw4; 303 ha) was constructed in late 2013 after being under continuous corn cultivation. Since the initial flooding, the wetland had filled in with tule (*Schoenoplectus acutus*) and cattail (*Typha* spp.) and represented an early-intermediate stage of restoration, with limited patches of open water. Mayberry restored wetland (US-Myb; 121 ha) was constructed in 2010 on Sherman Island, and represented an intermediate stage of restoration, with a similar species mix. With a water level as deep as 2 m in open-water channels, Mayberry wetland was the most heterogeneous of the four restored wetland treatments. Additionally, rising salinity levels in the wetland caused lowered productivity between 2014–2016. West Pond restored wetland (US-Tw1; 3 ha) was constructed in 1997 on Twitchell Island (Miller et al., 2008). Our eddy flux measurements began in summer 2012. West Pond, which was dominated by tall, emergent tule and cattail, represented a mature restored wetland and had no open water patches.

All restored wetland sites have undergone ‘wet’ restoration, a specific type of restoration in which the water table is actively managed to keep the wetland impounded year-round, preventing tidal, seasonal, or geomorphological input of sediment that natural wetlands would have received. Differing bathymetry and pumping schemes, as well as seasonal drought, cause slight variations in the water depth and quality at the four restored wetlands studied. Regenerative tule and cattail seeding was performed at select sites to promote canopy establishment. Due to the widespread modifications throughout the Delta, these novel

ecosystems may be more accurately understood of as ‘rehabilitated’ wetlands - sharing common hydrological conditions and species with their pre-industrial predecessor, but in no way biogeochemically or ecologically identical (Hemes et al., 2018a).

The agricultural sites included most of the dominant agricultural land uses in the Delta region: rice, pasture, corn, and alfalfa. Twitchell rice (US-Twt; *Oryza sativa*) was actively measured between 2009–2017 and planted on degraded, subsided peat soil (Knox et al., 2016). Sherman pasture (US-Snd), active between 2007–2015 (2010–2015 used in this study), was a pepperweed-dominated (*Lepidium latifolium* L.) pasture on the subsided peat soil that became Sherman wetland (Hatala et al., 2012; Teh et al., 2011). Corn (*Zea mays*) was measured during 2012–2013 on Twitchell Island on the location that became East End wetland in 2014, and during 2017 on Bouldin Island (US-Bi2) which contained higher soil C than the Twitchell corn site. Alfalfa (*Medicago sativa* L.) shares a perennial life-cycle strategy with the dominant wetland species and represents one of the largest water users in California (Hanson et al., 2007). This study incorporated data from alfalfa sites on Twitchell and Bouldin islands. Twitchell alfalfa (US-Tw4) was a seven year-continuously planted alfalfa field, previously planted in corn (Baldocchi and Sturtevant, 2015; Oikawa et al., 2016b). The site was sub-irrigated, harvested between 5 and 7 times a year, beginning in mid-March, and periodically grazed with sheep. Rapid leaf area index (LAI) changes (between ~1–3) due to an intensive harvest schedule greatly affected the GHG fluxes. Bouldin alfalfa (US-Bi1) was planted on a higher C soil than that on Twitchell Island, and was measured since August 2016 (Table S1).

2.2. Eddy covariance measurements and processing

The heterogeneous and continuous nature of ecosystem GHG emissions requires long-term spatially integrated measurements to fully characterize temporal and spatial variability (Baldocchi, 2003). We used the eddy covariance technique (Baldocchi et al., 1988) to capture continuous, long-term exchange of CO₂, CH₄, H₂O, and energy fluxes between the landscape and the atmosphere, along with measurements of environmental drivers (Eichelmann et al., 2018). Fluxes were measured by sampling a suite of sensors at a frequency of 10 (before ~2015) or 20 Hz, using open-path infrared gas analyzers (LI-7500 or LI-7500 A for CO₂ and H₂O, LI-7700 for CH₄, LiCOR Inc., Lincoln, NE, USA) that were calibrated every 3–6 months in the lab. Sonic anemometers measured sonic temperature and three-dimensional wind speeds at 20 Hz (WindMaster Pro 1352 or 1590, Gill Instruments Ltd, Lymington, Hampshire, England). The instrument setup (sampling rate, sensor separation, fetch and sensor height) was designed to minimize spectral loss (Detto et al., 2010). Typical cospectra exhibited slopes that closely match the idealized slope from Kaimal et al (1972). The main complication affecting the interpretation of our fluxes was the relative lack of homogeneity of the footprint of the restored wetlands, a mosaic of open water and vegetation (Eichelmann et al., 2018; Hemes et al., 2018b). Energy balance closure for many of these sites has been reported before and is adequate; non-closure at the wetland sites with large tracts of open water (Sherman, East End, and Mayberry wetlands) is due to the inability to capture the vertical and horizontal spatial variability in water column storage of the flux footprint, an important component of the energy balance (Eichelmann et al., 2018; Hemes et al., 2018b).

Trace gas and energy fluxes were calculated using the 30-minute covariance of turbulent fluctuations in vertical wind velocity and scalar of interest after applying a series of standard corrections and site-specific factors (Detto et al., 2010; Hatala et al., 2012; Knox et al., 2015). Coordinate rotations were performed so that mean wind velocities at each 30-minute averaging interval were zero in the cross-wind and vertical directions. To account for air density fluctuations sensed by the open path CH₄ and CO₂ sensors, the Webb-Pearman-Leuning corrections were applied (Chamberlain et al., 2017; Webb et al., 1980). To remove flux data measured over non-ideal conditions, half hourly fluxes

were filtered for stability and turbulence, friction velocity, wind direction, spikes in mean densities, variances and covariances, and sensor window obstruction.

To integrate yearly C and GHG budgets we gap filled fluxes by training an Artificial Neural Network (ANN) using measured meteorological variables (Dengel et al., 2013; Moffat et al., 2007; Papale et al., 2006). Training, validation, and testing data was selected from a series of k-means clusters to avoid seasonal or diel bias using Matlab 2017b software (Mathworks, Inc. 2012). Network architecture with varying levels of complexity were tested, with the simplest architecture selected for which further increases in complexity yielded less than a 5% reduction in mean standard error (Knox et al., 2016, 2015). This entire ANN procedure was performed 20 times, producing 20 separate ANNs. The median prediction of the 20 ANNs was used to fill gaps in the annual data.

Due to measurement periods not aligning with calendar years in the case of the two corn sites, we ‘wrapped’ a few months of the following year’s fluxes onto the previous year to achieve an annual calendar year timeseries and budget. This assumes that there is little interannual variability at a single corn site, which is reasonable considering the intensive management and precision farming practices employed. In addition, the wrapped fluxes were from early season (January to April) when the fields are largely fallow. For Bouldin corn, we appended fluxes from the first four months of 2018 to the 2017 record, which did not start until late April of that year. For Twitchell corn, we wrapped just over four months of 2013 to the 2012 record, which began in early May 2012. The tower was moved ~1 km in May of 2013 to make way for construction of East End wetland. To calculate the remaining two weeks necessary to get an annual sum, we extended the ANN predictions using meteorological data from the displaced tower site. These meteorological inputs do not differ significantly due to the close spatial proximity.

To investigate component fluxes at each site, we partitioned NEE into ecosystem respiration (R_{eco}) and gross primary productivity (GPP) using ANNs to predict daytime R_{eco} from nighttime measurements, when photosynthesis is inactive. The residual of NEE and daytime R_{eco} is the GPP. This method, while data-driven and avoiding assumptions of functional relationships between environmental drivers and component fluxes, does have drawbacks. It assumes that nighttime R_{eco} generally functions similarly to daytime R_{eco}, and has been shown to overestimate GPP and R_{eco}, potentially due to its inability to capture the Kok effect (Heskel et al., 2013; Oikawa et al., 2016b). For a global comparison analysis, we produced monthly sums from Fluxnet 2015 daily subset data (<http://fluxnet.fluxdata.org/>), excluding data with NEE quality control of less than 70%, and considering only months with complete daily data.

2.3. Carbon and greenhouse gas budgets

Net ecosystem carbon balance (NECB) was computed from the integrated annual sum of NEE (C – CO₂), and CH₄ (C – CH₄), as measured by continuous eddy covariance after quality control and gap filling as described above. For agricultural sites, removed, harvested biomass was added to the C budget. As the harvested crops of the Delta are commodities, the fate of their removed biomass is challenging to track with precision. Much of it may contribute to livestock feed, in which case it could partly result in enteric fermentation and additional CH₄ emissions. We follow a conservative approach and convert the removed biomass into CO₂ emissions for the purposes of the field-scale GHG accounting. A life-cycle accounting approach would more fully integrate the GHG fate of harvest, potentially resulting in larger GHG emissions at decadal timescales due to the decomposition of this biomass.

Harvest values were determined based on field-level farmer records where possible (Table 1). Rice harvest was taken from Knox et al. (2016), assuming dry rice grain contains 43% C. Harvest from the 2016

Table 1

Mean annual component GHG fluxes, harvest, net ecosystem carbon balance (NECB), GHG budget using global warming potential (GWP-28), sustained global warming potential (SGWP-45), and including N₂O (GWP-265, for the two sites for which it was measured). Uncertainty in component GHG fluxes and harvest is reported with standard error of annual sums (*or in the case of a site with a single year record, error from ANN and random error). NECB and GHG budget uncertainty is reported as propagated standard errors. ‘All wetland sites’ include all complete wetland site years. ‘All vegetated site-years’ excludes the first year of restoration at Sherman, East End, and Mayberry wetlands, before vegetation established. The symbol ‘n/a’ indicates that a field is not applicable to a particular site, while ‘-’ indicates that a value was not measured, and is assumed to be de minimis. **Due to only a single year of N₂O, no uncertainty in interannual variability of annual sums was included.

Site	CO ₂ g C-CO ₂ m ⁻² yr ⁻¹	CH ₄ g C-CH ₄ m ⁻² yr ⁻¹	Harvest g C m ⁻² yr ⁻¹	NECB	GWP		
					g CO ₂ eq m ⁻² yr ⁻¹	SGWP	GWP w/ N ₂ O
					CH ₄ GWP-28	CH ₄ GWP-45	CH ₄ GWP-28; N ₂ O GWP-265
Sherman wetland	324 ± 34*	46 ± 1*	n/a	370 ± 34*	2901 ± 124*	4111 ± 128*	-
East End wetland	-321 ± 202	32 ± 7	n/a	-290 ± 202	13 ± 782	852 ± 846	-
Mayberry wetland	-223 ± 79	50 ± 5	n/a	-173 ± 79	1060 ± 337	2385 ± 402	-
West Pond wetland	-454 ± 89	45 ± 4	n/a	-409 ± 89	32 ± 357	1228 ± 404	-
all wetland sites	-282 ± 73	44 ± 4	n/a	-238 ± 74	620 ± 292	1785 ± 328	-
all vegetated site-years	-386 ± 55	47 ± 4	n/a	-339 ± 55	333 ± 230	1565 ± 272	-
Twitchell rice	126 ± 115	12 ± 2	222 ± 14	360 ± 116	1735 ± 428	2059 ± 433	-
Sherman pasture	306 ± 36	9 ± 2	-	315 ± 36	1460 ± 146	1700 ± 168	-
Twitchell corn	292 ± 37*	-	293 ± 68*	585 ± 77*	2143 ± 281*	2143 ± 281*	-
Bouldin corn	826 ± 84*	2 ± 1*	712 ± 164*	1541 ± 184*	5719 ± 674*	5777 ± 675*	6595 ± 674**
Twitchell alfalfa	-249 ± 61	-	715 ± 150	466 ± 162	1709 ± 591	1709 ± 591	-
Bouldin alfalfa	-396 ± 90*	1 ± 3*	595 ± 137*	200 ± 164*	775 ± 607*	808 ± 619*	915 ± 607**

growing season, for which no record exists, was assumed to be the mean of the previous six years. Removed biomass from pasture was not quantified and assumed to be zero. Including it would make the pasture site a larger emission source. Twitchell corn harvest was from farmer records (Knox et al., 2015). Bouldin corn and alfalfa records were taken from farmer records, assuming 44% C dry matter, with corn harvested at 65% moisture and alfalfa at 88% moisture. For Twitchell alfalfa, we established annual relationships (linear least squares regression) between days since harvest and C sequestration measured from eddy covariance data to estimate total removed biomass at each cutting, and for each year. The mean value (715 ± 150 g C m⁻² yr⁻¹) falls between the upper and lower range given by the farmer.

Wetland NECB was composed primarily of photosynthetic inputs of CO₂ minus both autotrophic and heterotrophic respiration outputs of CO₂ and efflux of microbial CH₄. Because the wetlands were impounded, with little current and outflow, allochthonous lateral transport of dissolved C was not measured, and assumed to be negligible. In other more natural wetland systems, this lateral import and export of carbon is certainly an important component of the C balance (Chu et al., 2015; Krauss et al., 2018). By measuring NEE using the eddy covariance method, the dominant C inputs and outputs are measured continuously, and integrated over an entire footprint. At sites with negative NECB, the residual C was considered stored in the system.

To understand the impact of N₂O emissions on the GHG budget, continuous measurements of N₂O were conducted by an automatic flux chamber system installed in parallel at both the Bouldin corn and Bouldin alfalfa sites. Nine automated flux chambers (Eosense, Inc., Dartmouth, NS, Canada) were connected to a multiplexer, which dynamically signaled chamber deployment and routed gases to a Cavity Ring-Down Spectroscopy gas analyzer (Picarro, Santa Clara, CA, USA). Only one chamber was measured at a time, and each measurement took approximately 13 min. To reduce over- or under-estimation from individual chamber down-time, N₂O flux measurements were estimated using linear interpolation between consecutive measurements for each chamber. Fluxes were then averaged across all chambers over the measurement period (January 2017–January 2018 for Bouldin alfalfa; June 2017–June 2018 for Bouldin corn) to calculate annual N₂O flux (Anthony et al., in prep).

GHG budgets were computed from the integrated annual sum of NEE and emissions of CH₄, weighted according to GWP. Traditional GWP metrics were designed for a pulse emission but have been widely

applied to ecosystems and are the common standard in climate and emission accounting policies like California’s Cap and Trade system and the Kyoto Protocol. The ease and transparency with which these metrics can be applied have afforded them widespread adoption, despite well-documented inadequacies (Allen et al., 2016; Balcombe et al., 2018). Sustained global warming (and cooling) potential (SGWP) metrics account for the sustained nature of ecosystem emissions and differentiate between the effects of uptake and emission of important short-lived climate pollutants (SLCPs) (Neubauer and Megonigal, 2015). This SGWP metric has been applied to wetland sites previously (Hemes et al., 2018a; Krauss et al., 2016; Neubauer and Megonigal, 2015). We chose the IPCC AR5 GWP (without climate change feedbacks) for CH₄ of 28 CO₂eq and for N₂O of 265 CO₂eq (Myhre et al., 2013), and the SGWP for CH₄ of 45 CO₂eq (Neubauer and Megonigal, 2015), as these lie at the lower and upper end of commonly utilized cumulative 100-year warming potential metrics (Balcombe et al., 2018).

The GWP* metric has been shown to better track the temperature impacts of the integrated radiative forcing associated with SLCPs, which achieve steady state long before the conventionally assessed 100-year timeframe (Allen et al., 2018, 2016). Modeling of the GWP* metric provides a compelling alternative to adopting a standard but arbitrary amortization period like 100 years, as is necessary with GWP and SGWP metrics. To calculate GWP*, we used the method of Allen et al. (2016) where changes in CH (ΔCH₄) were accounted for instead of the magnitude of CH₄ (assuming a GWP of 28 CO₂eq). Mean grouped land use (wetland, corn, pasture, and alfalfa) CO₂ and CH₄ fluxes were used as inputs, with interannual variability as measured from our eddy covariance sites. We ran a Monte Carlo simulation (n = 1000) to capture the variability in switchover times due to the interannual variability in fluxes and present a mean year since restoration with a range of uncertainty (± 1 standard deviation) as the switchover time. Switchover time is defined as the length of time after which the positive radiative forcing due to increases in CH₄ emissions at a restored wetland is overtaken by the cumulative negative radiative forcing due to CO₂ uptake; when cumulative GHG emissions reach zero.

2.4. Uncertainty and error propagation

Uncertainty associated with annual NEE and CH₄ sums was estimated from both random half-hourly measurement error and ANN gap-filling error. For measured half hours, draws from a Laplace distribution

parameterized by the residuals of the ANN predictions (binned by flux magnitude) was used as an estimate of the random error (Moffat et al., 2007; Richardson and Hollinger, 2007). For gap-filled half hours, the variance of the cumulative sum of the 20 ANN predictions was used as a measure of uncertainty (Anderson et al., 2016; Knox et al., 2018). Adding the cumulative and random measurement uncertainties in quadrature resulted in the total uncertainty reported as 95% uncertainty intervals alongside annual sums. This uncertainty describes how well, given the missing data and random error associated with the method, we are able to predict a single year's NEE or CH₄. It does not consider any systematic errors intrinsic to the measurement technique and gap filling method.

We also calculated the mean annual sum of a specific site, across all years observed, or across a single land use type, across all site-years observed, to determine the average NEE or CH₄ fluxes (Table 1). Uncertainty for this quantity is reported as a standard error of the multiple annual sums, which considers the number of years measured (Table 1). In the case of Twitchell corn, Bouldin corn, and Bouldin alfalfa, where there is only a single site-year of data and thus no interannual standard error, we report the annual ANN and random error, which is commonly less than the error associated with interannual variability. Calculating uncertainty around mean site and land-use NECB, GWP, and SGWP values was done by adding, in quadrature, the standard error of the component fluxes (NEE, CH₄, and harvest, where applicable). Multi-year site and land-use mean NECB, GWP and SGWP therefore are reported with propagated uncertainty that represents how well we are able to predict this mean value based on the limited annual measurements we have, and not the measurement error, which tends to be much lower than error associated with year to year variation.

For sites with multiple years of harvested biomass, we take the interannual standard error. When only a single year of harvest was available (Twitchell corn, Bouldin corn, and Twitchell alfalfa), we assumed a standard deviation that is 23% of the measured harvested carbon. This error percentage was estimated from the difference between yield reported by the farmer, and that computed from field-level biomass samples taken near peak biomass at Bouldin corn. Because only one single year of N₂O chamber fluxes exist at two sites, we have no estimate of variation in multiyear sums, and thus exclude this in the error propagation at those two sites. All uncertainties are conservatively rounded up to the nearest whole number.

3. Results and discussion

3.1. Wetland land cover types

The wetlands exhibited regular seasonal variations in CO₂ flux, with net CO₂ uptake (negative NEE) during the growing season and net respiration (positive NEE) during the winter months (Fig. 1a, Fig S3 with confidence intervals). Except for the initial year after restoration, cumulative sums of NEE were neutral or negative (Fig. 2), indicating net annual uptake of CO₂ by the restored wetlands. Cumulative sums reach up to $-704 \pm 72 \text{ g C-CO}_2 \text{ m}^{-2} \text{ yr}^{-1}$ (West Pond, 2017; mean \pm annual 95% uncertainty) with site averages of -321 ± 202 , -223 ± 79 and $-454 \pm 89 \text{ g C-CO}_2 \text{ m}^{-2} \text{ yr}^{-1}$ (mean \pm interannual standard error) at East End, Mayberry and West Pond wetlands, respectively (Table 1).

Succession and disturbance caused large variation in NEE, and modulated the typical annual cycle of the established wetlands. The initial year after flooding, for which data exists at Sherman, East End, and Mayberry wetlands, were neutral to net sources. At that time, vegetation has not yet established and respiration from recently flooded soil contributed to a positive NEE for these three site-years of 201 ± 101 (Table 1; mean \pm interannual standard error). Sherman Wetland was a net CO₂ source during the 2017 growing season due to sparse vegetation throughout the measurement footprint (Fig. 2a). Similarly, East End's inaugural 2014 growing season was characterized by

net emissions of CO₂ as wetland vegetation slowly established, making the site a source of GHG (Fig. 2b). Mayberry wetland, restored in 2010, also experienced insect infestation (2013) and salinity stress (2015–2016), which reduced CO₂ uptake to near neutrality in those years (Fig. 2c). West Pond wetland, the most mature site (restored in 1997), exhibited perennial uptake (Fig. 2d) but lags other sites with a delayed green-up in the spring due to a thick layer of dead biomass that competes for photons and delays emergence (Eichelmann et al., 2018; Goulden et al., 2007) (Fig S2a).

Despite interannual variability, Delta wetlands were generally larger CO₂ sinks than other restored wetlands in the literature, especially those in cooler temperate and boreal climates. A rewetted bog in British Columbia was a modest CO₂ sink ($-179 \pm 26.2 \text{ gC-CO}_2 \text{ m}^{-2} \text{ yr}^{-1}$) 8 years after rewetting (Lee et al., 2016), while a restored wetland in Denmark, 7–9 years after rewetting, took up between -53 ± 8 and $-268 \pm 40 \text{ gC-CO}_2 \text{ m}^{-2} \text{ yr}^{-1}$ (Herbst et al., 2013). Another Danish restored riparian zone with periodic inundation was a net source of CO₂ ($220 \text{ g CO}_2\text{eq m}^{-2} \text{ yr}^{-1}$) 12 years after rewetting (Kandel et al., 2018). Mean uptake across all mature, vegetated wetland site-years in the Delta (not including initial years at Sherman, East End or Mayberry wetlands) was $-386 \pm 55 \text{ gC-CO}_2 \text{ m}^{-2} \text{ yr}^{-1}$ (Table 1). The high productivity in the Delta, driven by long growing seasons, warm temperatures, large macrophyte vegetation (~3 m tall), and managed water levels that inhibit aerobic soil respiration, came at a cost. Flooding also caused large CH₄ emissions during the growing season when soil and water temperatures were high and carbon from photosynthetic uptake was exuded into the rhizosphere (Fig. 3).

Delta wetland sites are among the highest CH₄ emitters across similarly measured wetlands around the world (Hemes et al., 2018a). CH₄ fluxes peaked in the summer and fell off throughout the winter as water temperatures decreased and GPP ceased (Fig. 3, S1b). Cumulative annual sums at the wetland sites ranged from 16 ± 1 to $63 \pm 2 \text{ g C-CH}_4 \text{ m}^{-2} \text{ year}^{-1}$ (Fig. 3; mean \pm annual 95% uncertainty), with an average across all wetland sites of $44 \pm 4 \text{ g C-CH}_4 \text{ m}^{-2} \text{ year}^{-1}$ (mean \pm interannual standard error).

Interannual variability, however, caused nearly two-fold differences in annual CH₄ sums. Recent work points to potential redox controls on methanogenesis driving interannual variability, including iron reduction in the years directly following restoration on alluvial soils, before significant peat soil accretion can dominate the soil redox environment (Chamberlain et al., 2018), and inadvertent temporary water table drawdowns creating oxidized conditions. Drivers of methane variability are diverse, scale dependent, and site specific (Sturtevant et al., 2016), although recent empirical modeling approaches can capture a large degree of the variability in these flooded systems (Oikawa et al., 2016a).

3.2. Agricultural land cover types

Agricultural land use types in the Delta included both annual (rice, pasture, and corn) and perennial crops (alfalfa) that underwent very different lifecycles and management practices, largely driving variation in biogeochemical cycling (Fig. 1b). Rice, which was flooded for the winter and growing season, exhibited net CO₂ uptake during the flooded growth stages, when soil respiration was largely inhibited by anaerobic conditions (Fig. 4a). Winter flooding (for bird habitat) kept winter respiration low, until spring pre-harvest drainage caused a spike in CO₂ efflux. Similarly, a CO₂ efflux spike in the fall occurred during drainage for harvest and before the field was reflooded (Figs. 1b, 4a). Depending on the size of these CO₂ emissions in comparison with uptake during the growing season, rice was a net CO₂ source or sink, with cumulative annual sums that ranged from 547 ± 42 to $-313 \pm 59 \text{ g C-CO}_2 \text{ m}^{-2} \text{ year}^{-1}$ before considering harvested biomass removal (Fig. 4a; mean \pm annual 95% uncertainty). The rice site emitted an average of $12 \pm 2 \text{ gC-CH}_4 \text{ m}^{-2} \text{ year}^{-1}$ (mean \pm interannual standard error), which accounted for ~10% of its mean CO₂ emissions over

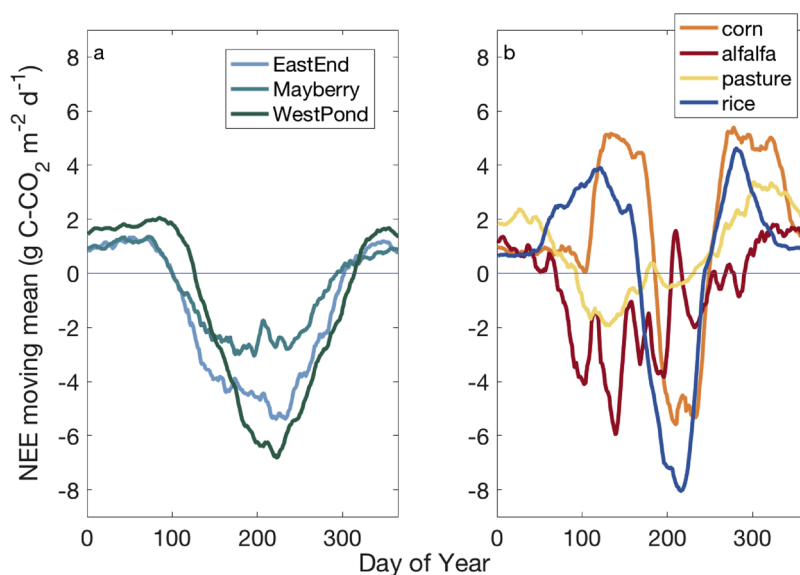


Fig. 1. Mean annual (10 day moving mean) net ecosystem exchange ($\text{g C-CO}_2 \text{ m}^{-2} \text{ d}^{-1}$) for a. wetland sites and b. agricultural sites for all complete site-years on record. Full timeseries for wetland sites and agricultural sites in Supplement (Figs S1, S2), as well as mean annual cycle with 95% uncertainty intervals (Figs S3, S4).

the study period. A CH_4 efflux spike occurred in the fall as the field was drained before harvest (Fig S2b), accounting for a large portion of the annual CH_4 sum.

Pasture was intermittently grazed, on subsided land with lower soil C stocks and periodic inundation (making it unfit for cropland). It contained the least amount of aboveground biomass, and thus exhibited low net uptake during the growing season (Fig. 1b). This uptake occurred in late spring, when invasive pepperweed was in growth stages. Over the hot, dry summer, growth trailed off, although pepperweed was able to tap subsurface irrigation or shallow groundwater due to the heavily subsided island. Large efflux spikes often corresponded to fall precipitation, when otherwise dry soil layers were moistened and microbial activity was catalyzed (Hatala et al., 2012) (Fig S2a). All years of data for the pasture site (2010–2014) resulted in a mean CO_2 source of $306 \pm 36 \text{ g C-CO}_2 \text{ m}^{-2} \text{ yr}^{-1}$ (mean \pm interannual standard error; Fig. 4b). Periodic anaerobic conditions from standing water after winter precipitation events evolved $9 \pm 2 \text{ gC-CH}_4 \text{ m}^{-2} \text{ yr}^{-1}$ (mean \pm interannual standard error) over the study period, accounting for a small portion of the pasture site's C budget (Table 1).

A single year of fluxes at two different corn sites (Twitchell corn, 2012–2013 and Bouldin corn, 2017–2018) showed strong growing season uptake during a two-month period (July–August) of rapid biomass accrual with large net respiration during other times of the year, except during flooding (December–February for bird habitat) in the winter (Fig. 1b). The Twitchell corn site respired less and also took up less CO_2 as compared to Bouldin corn, but both underwent peak uptake between DOY 200 and 250. The efficient C4 photosynthetic pathway of corn, achieving high LAI very rapidly, led to a relatively short period of net C uptake compared to the perennial wetlands or alfalfa crops. Despite high maximum uptake, the corn sites were net sources of CO_2 on an annual basis, even before accounting for harvested biomass emissions, of 292 ± 37 and $826 \pm 84 \text{ g C-CO}_2 \text{ m}^{-2} \text{ yr}^{-1}$, respectively (mean \pm annual 95% uncertainty; Fig. 4c,d). We measured low CH_4 emissions at Bouldin corn, primarily occurring during the flooded winter period, of $2 \pm 1 \text{ gC-CH}_4 \text{ m}^{-2} \text{ yr}^{-1}$ (Fig. S2b).

Alfalfa, a perennial crop, exhibits a much longer growing season than the annual crops, but is harvested multiple times a year, explaining the 5–6 periods of reduction in uptake during growing season cuttings

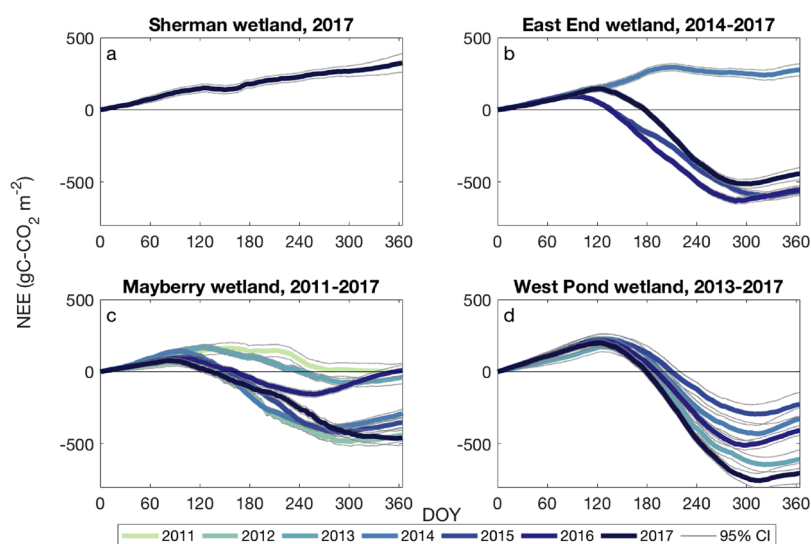


Fig. 2. Wetland site cumulative annual net ecosystem exchange ($\text{gC-CO}_2 \text{ m}^{-2} \text{ s}^{-1}$), with 95% uncertainty interval error bars from ANN and random error, in grey. (For interpretation of the references to colour in this figure legend, the reader is referred to the web version of this article).

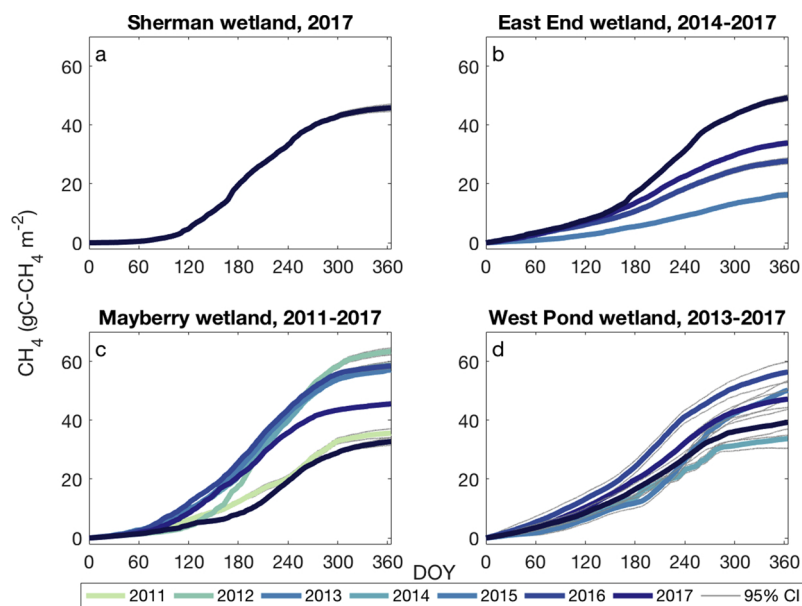


Fig. 3. Wetland site cumulative annual methane flux ($\text{gC-CH}_4 \text{ m}^{-2} \text{ s}^{-1}$), with 95% uncertainty interval error bars from ANN and random error, in grey. (For interpretation of the references to colour in this figure legend, the reader is referred to the web version of this article).

(Fig. 1b). Successive harvests resulted in incrementally lower uptake throughout the growing season. Before accounting for harvested biomass emissions, Twitchell alfalfa, planted on lower C soil, was a mean CO_2 sink of $-249 \pm 61 \text{ g C-CO}_2 \text{ m}^{-2} \text{ yr}^{-1}$ (mean \pm interannual standard error), while Bouldin alfalfa was a CO_2 sink of $-396 \pm 90 \text{ g C-CO}_2 \text{ m}^{-2} \text{ yr}^{-1}$ (Fig. 4e and f), with negligible CH_4 emissions ($1 \pm 3 \text{ g C-CH}_4 \text{ m}^{-2} \text{ yr}^{-1}$; mean \pm annual 95% uncertainty; Table 1).

3.3. Carbon and GHG budgets

To assess the potential for restored wetlands to sequester C compared to the drained agricultural land uses, we computed multi-year NECB. Except for the first year of restoration at Sherman wetland and East End wetland, NECB for the wetland sites was consistently neutral to negative, supporting our hypothesis that wetlands sequester C from the atmosphere and store it in accreted, organic soil (Fig. 5). This

accretion of C in wetland soils is confirmed by 4,000–6,000 years of historic peat buildup (Drexler et al., 2007; Weir, 1950), as well as recent accretion measurements at West Pond. Simulations suggest accretion of $\sim 3 \text{ cm yr}^{-1}$ with rates up to 9 cm yr^{-1} in some locations (Deverel et al., 2014; Miller et al., 2008).

Agricultural sites, on the other hand, were consistently neutral to net C sources, losing C to the atmosphere, mostly in the form of ecosystem CO_2 respiration and harvested biomass, which we considered a CO_2 emission upon removal from the field (Table 1). This net loss of C from the landscape (Fig. 5) is consistent with observations of significant subsidence of agricultural lands in the Delta (Deverel et al., 2016; Weir, 1950). In the case of perennial alfalfa, biomass removed from the site through harvest turns the site from a net sink to a net source of C. On the other hand, productivity would likely not be as high without the periodic harvests, which promote rapid biomass regeneration.

Taking all wetland site-years across the various successional stages, we derived a combined emission factor (using GWP-28) of

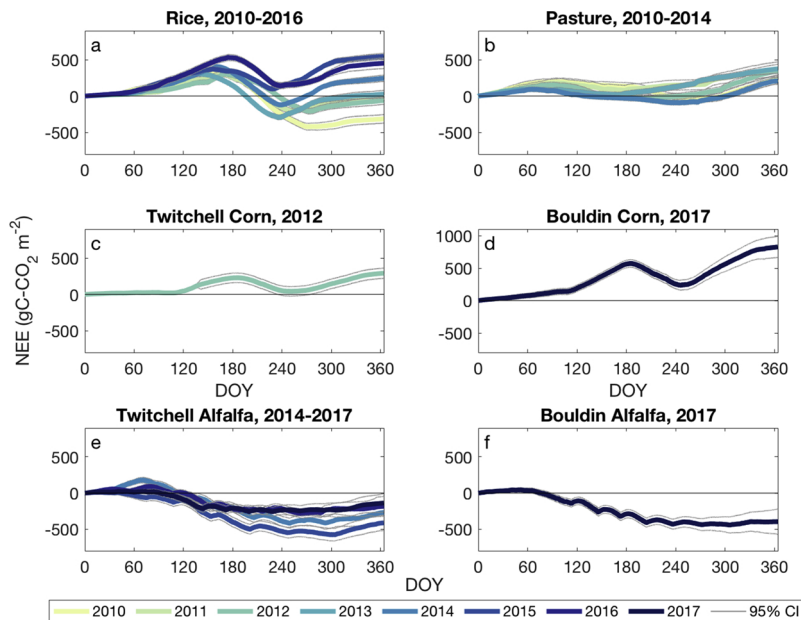


Fig. 4. Agricultural site cumulative annual net ecosystem exchange ($\text{gC-CO}_2 \text{ m}^{-2} \text{ s}^{-1}$), with 95% uncertainty interval error bars from ANN and random error, in grey. Sums are computed before considering removed biomass from harvest. (For interpretation of the references to colour in this figure legend, the reader is referred to the web version of this article).

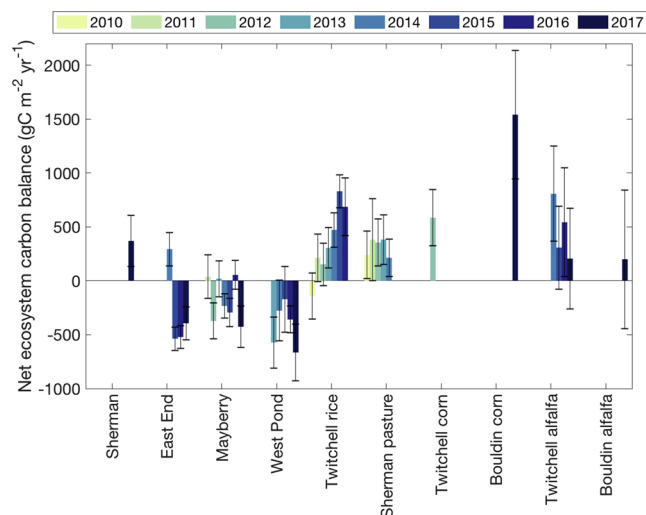


Fig. 5. Total annual net ecosystem carbon balance ($\text{g C m}^{-2} \text{yr}^{-1}$) for each full year at each site. Includes $\text{C}-\text{CO}_2$, $\text{C}-\text{CH}_4$, and C removed as harvested biomass from the agricultural sites. Error bars represent 95% uncertainty intervals of the ANN and random error.

$620 \pm 292 \text{ g CO}_2\text{eq m}^{-2} \text{yr}^{-1}$ (mean \pm propagated standard error) in the Delta (Table 1). This grows to $1785 \pm 328 \text{ g CO}_2\text{eq m}^{-2} \text{yr}^{-1}$ when using SGWP-45 metric for CH_4 . These values are not necessarily representative of future wetland emissions, as they are influenced greatly by the initial year after restoration, which is a large source. Mature, vegetated wetlands (excluding initial years after restoration) emitted, on average, $333 \pm 230 \text{ g CO}_2\text{eq m}^{-2} \text{yr}^{-1}$, using the GWP-28. For each individual site, annual CO_2eq emissions were positive for all land uses studied, regardless of GWP metric (Table 1). East End and West Pond wetlands were nearly neutral (13 ± 782 and $32 \pm 357 \text{ g CO}_2\text{eq m}^{-2} \text{yr}^{-1}$) assuming a GWP-28, while the recently or often disturbed wetlands, like Sherman and Mayberry, were in some cases larger emitters (2901 ± 124 and $1060 \pm 337 \text{ g CO}_2\text{eq m}^{-2} \text{yr}^{-1}$, respectively) than certain agricultural land uses. When the long-term radiative forcing impacts of CH_4 were given more weight due to their sustained nature, as with the SGWP-45 metric, the wetland GHG budgets increased and were, in some cases, larger than agricultural land uses with low CH_4 emissions. Agricultural sites were all net sources of CO_2eq , even before addition of the N_2O contribution, which was applied for the two sites at which it was measured, using the GWP-265 metric. The corn and rice sites were larger sources than the pasture and alfalfa sites, regardless of the GWP metric.

Beyond restored Delta wetlands, where freshwater inputs keep the water table above the land surface, long-term, continuous, ecosystem-scale accounting of GHG impacts of restored wetlands are limited. Due to geomorphology, climate, wetland type, and restoration strategy, there is considerable variability in emissions from restored peat wetlands (Hoper et al., 2008). A multiyear chamber study of the GHG budgets at a seven-year old restored freshwater bog in Ireland reported a significant net reduction in the GWP at the rewetted and colonized wetland site compared to a drained control, despite a net positive GWP at most revegetated sites (Wilson et al., 2016b). A rewetted British Columbia peat bog was nearly neutral using GWP-28 after almost a decade of re-wetting (Lee et al., 2016). A Dutch peatland landscape study found that agricultural drained peatlands could be returned to sinks of GHG and C within 15 years of rewetting (Schrier-Uijl et al., 2014), while a different restored wetland, 7–9 years after rewetting ranged from a large GHG sink to a small GHG source, both assuming GWP-25 (Herbst et al., 2013). Lack of consistent application of GWP values, as well as different ages and paces of succession, make comparisons between restored wetlands challenging. While our wetland sites are consistently C sinks, their GHG budgets are all positive due to

large CH_4 emissions (Table 1). In many cases, however, drained peat soil agricultural sites are equivalent or larger GHG sources.

Our continuous ecosystem-scale wetland and agricultural measurements capture the net impact of the dominant two GHGs – CO_2 and CH_4 . In the wetlands, redox states that support partial denitrification and evolution of N_2O are not common (Wilson et al., 2016a, 2016b), unless high NO_3^- inputs inhibit nitrous oxide reductase enzyme activity (Tiedje, 1988). Weekly ebullition chamber and dissolved N_2O measurements at Mayberry wetland confirmed that the contribution of N_2O to radiative forcing was negligible, compared to the other two GHGs (McNicol et al., 2016). In Denmark, a rewetted temperate riparian wetland's annual N_2O emissions accounted for 7% of its overall GHG budget, although this could have been partially stimulated by the periodic inundation (Kandel et al., 2018).

At the agricultural sites, N_2O is not negligible due to nitrogen fertilization and fluctuating redox dynamics favorable to N_2O evolution during irrigation or precipitation (Firestone and Davidson, 1989). Using an array of nine automatic chambers co-located with our eddy covariance measurements at Bouldin corn and Bouldin alfalfa, we measured annual sums of $3.28 \pm 0.12 \text{ g N}_2\text{O m}^{-2} \text{yr}^{-1}$ and $0.51 \pm 0.07 \text{ g N}_2\text{O m}^{-2} \text{yr}^{-1}$ (mean \pm standard error), respectively (Anthony et al., in prep). Using the 100-year GWP of $265 \text{ g CO}_2\text{eq}$, radiative forcing due to N_2O accounted for 15% and 17% of these agricultural sites' annual GHG budget, or 868 and $135 \text{ g CO}_2\text{eq m}^{-2} \text{yr}^{-1}$ (Table 1). A literature review by Deverel et al. (2017) estimates that agriculture N_2O in the Delta amounts to between $262\text{--}974 \text{ g CO}_2 \text{eq m}^{-2} \text{yr}^{-1}$. IPCC Tier 1 emission factors for N_2O are on the order of $609 \text{ g CO}_2\text{eq m}^{-2} \text{yr}^{-1}$ (Wilson et al., 2016a). N_2O emissions of this order of magnitude warrant further continuous measurements of this important GHG.

3.4. Climatic impact of restoration

Conversion from a large GHG source land use type, like Bouldin corn, to a restored wetland, always yields an emission reduction over a 100-year timescale, no matter the GWP metric used (Table 2). Other land use conversions, like those from pasture to wetland, will conditionally yield a net emission reduction, depending on the biogeochemical performance and management of the specific restored wetland, as well as the GWP metric considered. Conversion from Twitchell corn and Twitchell alfalfa are similar – if transitioning to a restored wetland like East End or West Pond, emission reductions are achieved, no matter the GWP metric. If transitioning to a wetland like Mayberry, the GWP metric chosen will determine if emission reductions are achieved. Conversion from agricultural systems that are net GHG sinks, like Bouldin alfalfa (and only small net sources after harvest is considered), may in some cases yield emission increases over a 100-year timescale according to these metrics. If considering the agricultural sites' N_2O burden, which we omitted from Table 2 as it was not measured consistently across sites, potential emission reductions from wetland restoration would increase.

In systems that produce considerable SLCPs, like the restored wetlands studied here, the timescale of analysis can influence the apparent climate impact of the land use change. Much previous work in natural wetlands has shown that despite CH_4 emissions, over multi-century timescales natural wetlands tend to have a net biogeochemical cooling effect (Frolking and Roulet, 2007; Roulet, 2000; Roulet et al., 2007). Over time, the cumulative removal of CO_2 , an extremely long-lived GHG, vastly outweighs the short-lived CH_4 warming effect. Discrepancies between GWP metrics utilized to equate CH_4 with CO_2 greatly affect if and when emission reductions are achieved and the quantity of those net reductions (Table 2). The debate continues about how to best account for SLCPs like CH_4 in the context of land-use changes, technology assessments, and mitigation scenarios at the national scale (Allen et al., 2018; Balcombe et al., 2018; Neubauer and Megonigal, 2015). Recent CH_4 emissions may be especially important to short-term climate forcing, as the post-2006 uptick in atmospheric

Table 2

Matrix of emission reductions (blue) or increases (red) in a theoretical land use transition from agricultural (columns) to flooded land uses (rows) in g CO₂ eq m⁻² yr⁻¹ assuming a GWP of 28 (upper; Myhre et al., 2013) and a SGWP of 45 (bottom; Neubauer and Megonigal, 2015). Emissions from N₂O not included, as these were only measured for two site-years. Uncertainty is reported as propagated standard error of component CO₂, CH₄, and harvest, where applicable.

GWP 28	<i>Sherman Pasture</i>	<i>Twitchell Corn</i>	<i>Bouldin Corn</i>	<i>Twitchell Alfalfa</i>	<i>Bouldin Alfalfa</i>
<i>Sherman</i>	1441 ± 191	759 ± 307	-2818 ± 685	1193 ± 604	2126 ± 619
<i>East End</i>	-1448 ± 795	-2130 ± 831	-5707 ± 1032	-1696 ± 980	-762 ± 990
<i>Mayberry</i>	-400 ± 367	-1083 ± 439	-4660 ± 754	-649 ± 680	285 ± 694
<i>West Pond</i>	-1428 ± 385	-2110 ± 454	-5687 ± 763	-1677 ± 690	-743 ± 704
<i>Twitchell Rice</i>	274 ± 449	-408 ± 509	-3985 ± 797	26 ± 728	960 ± 741
SGWP 45	<i>Sherman Pasture</i>	<i>Twitchell Corn</i>	<i>Bouldin Corn</i>	<i>Twitchell Alfalfa</i>	<i>Bouldin Alfalfa</i>
<i>Sherman</i>	2411 ± 211	1968 ± 308	-1667 ± 687	2402 ± 604	3303 ± 632
<i>East End</i>	-849 ± 863	-1291 ± 892	-4926 ± 1082	-857 ± 1032	44 ± 1049
<i>Mayberry</i>	684 ± 436	242 ± 490	-3393 ± 785	676 ± 715	1576 ± 738
<i>West Pond</i>	-472 ± 437	-914 ± 491	-4549 ± 786	-480 ± 715	420 ± 739
<i>Twitchell Rice</i>	359 ± 465	-84 ± 516	-3718 ± 802	350 ± 732	1251 ± 756

CH₄ concentrations were associated with an immediate, positive trend in radiative forcing (Feldman et al., 2018). On the other hand, emerging metrics, like GWP*, emphasize the change in SLCFs' flux rate over the cumulative emissions, due to the short atmospheric lifetime of these gases (Allen et al., 2016).

With a simple GWP* model based on ΔCH₄, we assess the 'switch-over time' for which restored Delta wetland ecosystems transition from a source to a sink, e.g., when the positive radiative forcing associated with CO₂ respiration and CH₄ emissions is overtaken by the negative radiative forcing of CO₂ removal (Fig. 6). We also compute how many years it takes for wetland restoration to begin to accrue net GHG benefits to the atmosphere – this occurs when the cumulative wetland GHG emissions (black line) and the cumulative CO₂ emissions of the agricultural land use (orange, yellow, pink lines) cross (Fig. 6). Using these conventions, we compare the avoided emission trajectories of a land use transition from agriculture to a restored wetland, for three cases relevant to the Delta. Due to the abrupt change in NEE after the initial year of restoration, we model the initial year based on the mean and standard deviation of NEE and CH₄ emissions from year one at Sherman, East End, and Mayberry wetlands. Subsequent years are assigned the emission factor for NEE and CH₄ from fully vegetated wetlands, which excludes the initial year at those same sites (Table 1).

When transitioning from corn to wetland using the GWP* metric (Fig. 6a), the two land uses become GHG equivalent sources after 60 ± 16 (mean ± 95% uncertainty interval of crossover) years. After this time, the restored wetland begins to accrue a net GHG benefit to the atmosphere, compared to its preceding land use. The wetland's large initial CH₄ burden, incurred when transitioning from a drained to a flooded land use, incurs a sizeable GHG 'debt' that is only neutralized by its cumulative CO₂ uptake after 119 ± 30 years. At this switchover time, the wetland land use has saved 169 kg CO₂eq m⁻² compared to continuous corn, and will continue to be GHG beneficial into the future assuming stable environmental conditions and no major disturbances.

A wetland restored from pasture, which is a much smaller net source

than corn, will take 80 ± 24 years to begin accruing climate benefit. At the time the wetland switches over from a cumulative source to a cumulative sink (101 ± 31 years), it will have saved 42 kg CO₂eq m⁻² compared to continuous pasture land use (Fig. 6b). Because the low-lying pasture is already a CH₄ emitter, the ΔCH₄ 'debt' upon restoration is not as large, and thus the switchover time comes sooner than other land uses. Finally, a wetland restored from alfalfa will take 89 ± 22 years to begin accruing GHG benefits. After 124 ± 31 years, it will switchover to a net GHG sink, at which time it will have avoided 72 kg CO₂eq m⁻² compared to continuous alfalfa land use (Fig. 6c).

Despite a large range of uncertainty due to the sizeable interannual variability in annual restored wetland CO₂ and CH₄ fluxes, we can see that depending on the preceding 'baseline' land use, restored wetlands will begin to accrue GHG benefits after a half century, and become net sinks from the atmosphere after a century. Because our simulation uses the same 'representative' wetland for each scenario, the differences in the switchover time and CO₂ savings are attributed to the emission burden of the 'business-as-usual' agricultural land use. Multi-decadal permanence of this kind of wetland restoration may not be sufficient to ensure GHG benefits, due to the time it takes for the incurred CH₄ debt to be neutralized by CO₂ uptake. On a multi-century timescale, however, these wetland land uses can be seen as largely climate-beneficial.

Common carbon crediting schemes compare GHG emissions of a low-emission land-use activity to a 'business as usual' baseline over a multi-decadal timescale, typically using a 100-year GWP. Wetland restoration, for example, would be compared to the agricultural land use that preceded it to compute emission reductions (Table 2). This framework generally assumes a static baseline – that the agricultural emissions are constant through time. In the Delta, with increasing subsidence and reductions in surface C stocks over time, high-value agriculture is often transitioned to lower-value agriculture as the soil quality is diminished. Future work could more explicitly capture this in long term projections.

Similarly, little is known about the long-term successional trajectory

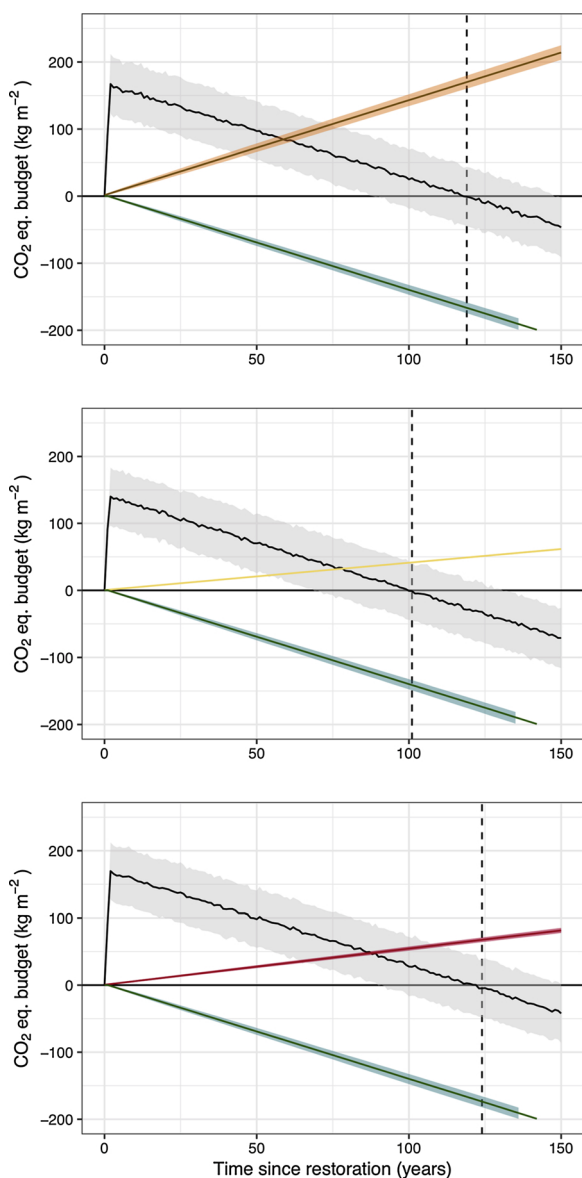


Fig. 6. Modeled cumulative wetland CO₂ uptake (green line) and cumulative net GHG emissions of CO₂ and CH₄ (black line) versus agricultural 'business as usual' cumulative CO₂ emissions for a. corn, b. pasture, and c. alfalfa. Emission rates based on mean annual land use fluxes reported above, using the GWP* metric of Allen et al., (2016 & 2018). Grey area represents 95% uncertainty in switchover time. (For interpretation of the references to colour in this figure legend, the reader is referred to the web version of this article).

of restored wetlands, which can be considered novel systems due to their unique hydrological management and land use history. Although theory from natural terrestrial ecosystems suggests that in late ecological succession, NEE would tend towards zero (Chapin et al., 2012; Odum, 1969), this may not be the case in highly managed systems, especially given that the most mature restored wetland (West Pond, restored 1997) often took up the most CO₂ annually (Fig. 2d). We assume that our sample of wetland site-years, which range from one to twenty years since restoration, is representative of the kinds of disturbance and interannual variability that may be encountered throughout a century. Our future projections are also limited due to uncertainties around future climate in California, which is likely to get hotter and drier throughout the century (Pathak et al., 2018). In addition to the biogeochemical considerations, commonly utilized quantification schemes rarely recognize the radiative and non-radiative

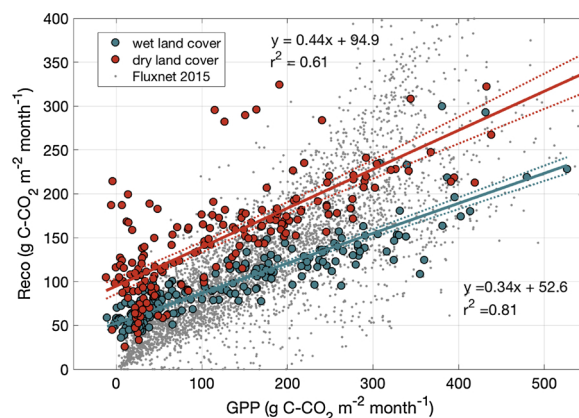


Fig. 7. Monthly sums of gross primary productivity ($\text{g C-CO}_2 \text{ m}^{-2} \text{ month}^{-1}$) and ecosystem respiration ($\text{g C-CO}_2 \text{ m}^{-2} \text{ month}^{-1}$) for aggregated land cover classes, with 95% uncertainty (dashed lines).

impacts associated with biophysical changes due to restoration such as albedo, roughness, and evaporative efficiency (Baldocchi and Panuelas, 2018; Bonan, 2008; Perugini et al., 2017). In the case of wetlands, the net biophysical forcings cause a surface cooling effect and a reduction in the diurnal temperature range compared to an agricultural 'baseline' (Hemes et al., 2018b).

3.5. Scaling implications

Using our 36 site-years of continuous ecosystem-scale measurements, we derived a relationship between GPP and ecosystem respiration (R_{eco}) in the Delta, aggregated by land use type (Fig. 7; see Fig. S6 for disaggregated relationships). Wetland land use types and flooded periods of rice – together 'wet land cover' – inhibited R_{eco} in a way that reduced the slope of the R_{eco} :GPP relationship by 23% compared to the 'dry' agricultural land covers, which did not generally have standing water. The background emissions in the absence of GPP were about half as much for the wet land covers ($52.6 \pm 1.9 \text{ g C-CO}_2 \text{ m}^{-2} \text{ month}^{-1}$; intercept \pm standard error) compared to the dry ($94.9 \pm 4.5 \text{ g C-CO}_2 \text{ m}^{-2} \text{ month}^{-1}$). This flooding-induced inhibition of soil respiration reduced the C loss of the restored wetlands, led to C sequestration and in many cases, GHG emission reductions in transitions from degraded agricultural peat soils to managed restored wetlands (Table 2).

Compared to the biogeochemical 'space' occupied by the range of biomes represented in the Fluxnet network of eddy covariance measurement sites across the world (Fig. 7; grey points), we see that high-productivity wet land cover months occupy the lower right edge of the figure. The Delta's 'dry' land cover sites – irrigated agricultural sites on drained, organic peat soils, displayed some of the higher monthly R_{eco} :GPP ratios across the network, especially during shoulder season periods of exposed soil but little productivity. Our sites' highly organic soils and raised water levels add unique parameter space to the previous understandings of R_{eco} :GPP ratios. These high ratios are especially apparent at our rice site, when drained, and at our Bouldin corn site, which is on soil with especially high C content (~18% C) (Fig S6). Conversion of these highly respiring sites to restored wetlands with vastly inhibited soil respiration can potentially achieve the greatest emission reductions. Observationally derived ratios of R_{eco} :GPP at a range of soil organic C content sites across the Delta could allow for spatial modeling of fluxes within a carbon accounting framework, as well as to identify restoration sites that would yield optimum GHG reductions.

While our network across the western and central Delta represents a range of dominant land uses over multiple years, scaling these field-level measurements to the broader Delta region will require a robust

measurement-based modeling framework. Modeling frameworks that have been validated on measured observations and can capture emissions from restored wetlands could be an important tool to reduce costs associated with measurement and verification (Oikawa et al., 2016a). Methodologies that are not based on direct measurement, and instead use conservative emission factors, can underestimate the potential emission reductions achieved, and thus jeopardize funding for restoration projects. Recent analysis of one of the first carbon credit projects transacted for peatland restoration found that direct measurements, as opposed to conservative emission factors, resulted in a greater number of carbon credits the majority of the time (Günther et al., 2018). These benefits must be weighed against the costs to project proponents of undertaking and directly measuring the effects of a restoration project. Simple models that can be validated and calibrated for specific geographies and soil types, and rely on publicly available and remotely sensed data inputs, have the best chance of balancing cost and scientific rigor at scale to promote land use activities within a market or payment-for-ecosystem services program.

4. Conclusion

Restoring drained and degraded peat soils to managed, impounded wetlands presents an attractive, but largely untested, climate change mitigation potential (Deverel et al., 2017; Griscom et al., 2017; Leifeld and Menichetti, 2018). Here, we synthesize 36 site-years of continuous CO₂ and CH₄ flux data from a mesonetwork of eddy covariance towers in the Sacramento-San Joaquin River Delta to compute C and GHG budgets for drained agricultural peatland sites and a chronosequence of four restored wetlands. Due to management practices that inhibit R_{eco} and allow for robust GPP (Fig. 7), we find that restored wetlands effectively sequester C, reversing soil loss that is associated with subsiding drained agricultural land uses (Fig. 5). After the initial year of restoration, wetland land uses were, on average, sizeable sinks of C ($-339 \pm 55 \text{ g C m}^{-2} \text{ yr}^{-1}$), while agricultural sites lost up to $1541 \pm 184 \text{ g C m}^{-2} \text{ yr}^{-1}$ (Bouldin Corn, 2017; Table 1).

CH₄ emissions due to anaerobic decomposition and lack of CH₄ oxidation result in wetlands being near neutral to GHG sources (Hemes et al., 2018a), although the choice of GWP metric has an important impact on the magnitude of the total GHG budget (Table 1). Despite this, depending on the successional age and disturbance regime of the restored wetland, many land use conversions from agriculture to restored wetland would result in emission reductions over a 100-year timescale (Table 2). With a simple model of radiative forcing and atmospheric lifetimes, we show that restored wetlands will not begin to accrue GHG benefits for at least a half century, and become net sinks from the atmosphere after a century or more (Fig. 6). Policymakers and planners should take measures that promote the long-term restoration of these kinds of systems to maximize climatic benefit. Chronosequences of restored wetlands must be continuously measured to understand how their GHG sink or source nature changes as they mature.

Simple models, based on measured relationships between partitioned fluxes (Fig. 7), could be instrumental in reducing costs and increasing implementation of GHG emission reduction projects like wetland restoration (Oikawa et al., 2016a). More robust integration of long-term N₂O fluxes into the GHG budgets of the agricultural sites will likely increase the net benefit of wetland restoration. Active wetland management to reduce CH₄ evolution, through water table and/or redox manipulation, could also increase the benefit of restoration (Hemes et al., 2018a). Potential biogeochemical benefits of restoration should be considered in light of the other important co-benefits, such as habitat, water infrastructure, and microclimate impacts (Hemes et al., 2018b). Long term, continuous, ecosystem-scale measurements of land-atmosphere exchange over a range of managed land uses, disturbance regimes, and soil types will contribute to our understanding of how policies and programs could incentivize low emission land use

management and climate change mitigation.

Acknowledgements

This work was supported by the California Department of Water Resources (DWR) through a contract from the California Department of Fish and Wildlife and the United States Department of Agriculture (NIFA grant #2011-67003-30371). Funding for the AmeriFlux core sites was provided by the U.S. Department of Energy's Office of Science (AmeriFlux contract #7079856).

KSH was supported by the California Sea Grant Delta Science Fellowship. This material is based upon work supported by the Delta Stewardship Council Delta Science Program under Grant No. 2271 and California Sea Grant College Program Project R/SF-70. The contents of this material do not necessarily reflect the views and policies of the Delta Stewardship Council or California Sea Grant, nor does mention of trade names or commercial products constitute endorsement or recommendation for use. KK was supported by the Baltic-American Freedom Foundation Research Scholar program.

The authors recognize the work of all Berkeley Biometeorology Lab members who helped maintain towers and collected and processed data over the lifetime of these sites, especially the undergraduate summer lab assistants. We thank the California Department of Water Resources and the Metropolitan Water District of Southern California for collaboration and access to research sites.

All Delta sites used in this analysis are part of the AmeriFlux network, with data available at <http://ameriflux.lbl.gov/>.

This work used eddy covariance data acquired and shared by the FLUXNET community, including these networks: AmeriFlux, AfriFlux, AsiaFlux, CarboAfrica, CarboEuropeIP, CarboItaly, CarboMont, ChinaFlux, Fluxnet-Canada, GreenGrass, ICOS, KoFlux, LBA, NECC, OzFlux-TERN, TCOS-Siberia, and USCCC. The ERA-Interim reanalysis data are provided by ECMWF and processed by LSCE. The FLUXNET eddy covariance data processing and harmonization was carried out by the European Fluxes Database Cluster, AmeriFlux Management Project, and Fluxdata project of FLUXNET, with the support of CDIAC and ICOS Ecosystem Thematic Center, and the OzFlux, ChinaFlux and AsiaFlux offices.

Appendix A. Supplementary data

Supplementary material related to this article can be found, in the online version, at doi:<https://doi.org/10.1016/j.agrformet.2019.01.017>.

References

- Allen, M.R., Fuglestedt, J.S., Shine, K.P., Reisinger, A., Pierrehumbert, R.T., Forster, P.M., 2016. New use of global warming potentials to compare cumulative and short-lived climate pollutants. *Nat. Clim. Chang.* <https://doi.org/10.1038/nclimate2998>.
- Allen, M.R., Shine, K.P., Fuglestedt, J.S., Millar, R.J., Cain, M., Frame, D.J., Macey, A.H., 2018. A solution to the misrepresentations of CO₂-equivalent emissions of short-lived climate pollutants under ambitious mitigation. *NPJ Clim. Atmos. Sci.* 1. <https://doi.org/10.1038/s41612-018-0026-8>.
- Anderson, F.E., Bergamaschi, B., Sturtevant, C., Knox, S.H., Hastings, L., Windham-Myers, L., Detto, M., Hestir, E.L., Drexler, J., Miller, R.L., Matthes, J.H., Verfaillie, J.G., Baldocchi, D.D., Snyder, R.L., Fujii, R., 2016. Variation of energy and carbon fluxes from a restored temperate freshwater wetland and implications for carbon market verification protocols. *J. Geophys. Res. Biogeosci.* <https://doi.org/10.1002/2015JG003083>. n/a-n/a.
- Anderson, M., Gao, F., Knipper, K., Hain, C., Dulaney, W., Baldocchi, D., Eichelmann, E., Hemes, K., Yang, Y., Medellín-Azuara, J., Kustas, W., 2018. Field-Scale Assessment of Land and Water Use Change Over the California Delta Using Remote Sensing 10. <https://doi.org/10.3390/rs10060889>.
- Atwater, B.F., Conard, S.G., Dowden, J.N., Hedel, C.W., MacDonald, R.L., Savage, W., 1979. History, Landforms, and Vegetation of the Estuary's Tidal Marshes, Pacific Division of the American Association for the Advancement of Science.
- Balcombe, P., Speirs, J.F., Hawkes, A.D., Brandon, N.P., 2018. Methane emissions: choosing the right climate metric and time horizon. *Environ. Sci. Process. Impacts* <https://doi.org/2018/EM/C8EM00414E>.
- Baldocchi, D.D., 2003. Assessing the eddy covariance technique for evaluating carbon

- diode exchange rates of ecosystems: past, present and future. *Glob. Chang. Biol.* 9, 479–492. <https://doi.org/10.1046/j.1365-2486.2003.00629.x>.
- Baldocchi, D.D., Panuelas, J., 2018. The physics and ecology of mining carbon dioxide from the atmosphere by ecosystems. *Glob. Chang. Biol.* <https://doi.org/10.1111/gcb.14559>.
- Baldocchi, D., Sturtevant, C., 2015. Does day and night sampling reduce spurious correlation between canopy photosynthesis and ecosystem respiration? *Agric. For. Meteorol.* 207. <https://doi.org/10.1016/j.agrformet.2015.03.010>.
- Baldocchi, D.D., Hicks, B.B., Meyers, T.P., Hincks, B.B., Meyers, T.P., 1988. Measuring biosphere-atmosphere exchanges of biologically related gases with micro-meteorological methods. *Ecology*. <https://doi.org/10.2307/1941631>.
- Bonan, G.B., 2008. Forests and climate change: forcings, feedbacks, and the climate benefits of forests. *Science* 320, 1444–1449. <https://doi.org/10.1126/science.1155121>.
- Bridgman, S.D., Cadillo-Quiroz, H., Keller, J.K., Zhuang, Q., 2013. Methane emissions from wetlands: biogeochemical, microbial, and modeling perspectives from local to global scales. *Glob. Chang. Biol.* 19, 1325–1346. <https://doi.org/10.1111/gcb.12131>.
- Canadell, J.G., Schulze, E.D., 2014. Global potential of biospheric carbon management for climate mitigation. *Nat. Commun.* 5, 5282. <https://doi.org/10.1038/ncomms6282>.
- Chamberlain, S.D., Verfaillie, J.G., Eichelmann, E., Hemes, K.S., Baldocchi, D.D., 2017. Evaluation of density corrections to methane fluxes measured by Open-Path Eddy Covariance over contrasting landscapes. *Boundary-Layer Meteorol.* 165, 197–210. <https://doi.org/10.1007/s10546-017-0275-9>.
- Chamberlain, S.D., Anthony, T.L., Silver, W.L., Eichelmann, E., Hemes, K.S., Oikawa, P.Y., Sturtevant, C., Szutu, D.J., Verfaillie, J.G., Baldocchi, D.D., 2018. Soil properties and sediment accretion modulate methane fluxes from restored wetlands. *Glob. Chang. Biol.* 24, 4107–4121. <https://doi.org/10.1111/gcb.14124>.
- Chapin, F.S., Matson, P.A., Vitousek, P.M., 2012. *Principles of Terrestrial Ecosystem Ecology*, 2nd ed. Springer, New York, NY.
- Chu, H., Gottgens, J.F., Chen, J., Sun, G., Desai, A.R., Ouyang, Z., Shao, C., Czajkowski, K., 2015. Climatic variability, hydrologic anomaly, and methane emission can turn productive freshwater marshes into net carbon sources. *Glob. Chang. Biol.* 21, 1165–1181. <https://doi.org/10.1111/gcb.12760>.
- Cloern, J.E., Jassby, A.D., 2012. Drivers of change in estuarine - coastal ecosystems: discoveries from four decades of study in San Francisco Bay. *Rev. Geophys.* 50, 1–33. <https://doi.org/10.1029/2012RG000397.1>. INTRODUCTION.
- Dean, J.F., Middelburg, J.J., Röckmann, T., Aerts, R., Blauw, L.G., Egger, M., Jetten, M.S.M., de Jong, A.E.E., Meisel, O.H., Rasigraf, O., Slomp, C.P., 't Zandt, M.H., Dolman, A.J., 2018. Methane feedbacks to the global climate system in a warmer world. *Rev. Geophys.* <https://doi.org/10.1002/2017RG000559>.
- Dengel, S., Zona, D., Sachs, T., Aurela, M., Jammet, M., Parmentier, F.J.W., Oechel, W., Vesala, T., 2013. Testing the applicability of neural networks as a gap-filling method using CH4 flux data from high latitude wetlands. *Biogeosciences* 10, 8185–8200. <https://doi.org/10.5194/bg-10-8185-2013>.
- Detto, M., Baldocchi, D.D., Katul, G.G., 2010. Scaling properties of biologically active scalar concentration fluctuations in the atmospheric surface layer over a managed peatland. *Boundary-Layer Meteorol.* 136, 407–430. <https://doi.org/10.1007/s10546-010-9514-z>.
- Deverel, S.J., Leighton, D.A., 2010. Historic, recent, and future subsidence, Sacramento-San Joaquin Delta, California, USA. *San Fr. Estuary Watershed Sci.* 8.
- Deverel, S.J., Ingrum, T., Lucero, C., Drexler, J.Z., 2014. Impounded marshes on subsided islands: simulated vertical accretion, processes, and effects, Sacramento-San Joaquin Delta, CA USA. *San Fr. Estuary Watershed Sci.* 12.
- Deverel, S.J., Ingrum, T., Leighton, D., 2016. Present-day oxidative subsidence of organic soils and mitigation in the Sacramento-San Joaquin Delta, California, USA. *Hydrogeol. J.* 24, 569–586. <https://doi.org/10.1007/s10040-016-1391-1>.
- Deverel, S.J., Jacobs, P., Lucero, C., Dore, S., Kelsey, T.R., 2017. Implications for greenhouse gas emission reductions and economics of a changing agricultural mosaic in the Sacramento - San Joaquin Delta. *San Fr. Estuary Watershed Sci.* 15. <https://doi.org/10.5811/westjem.2011.5.6700>.
- Drexler, J.Z., de Fontaine, C., Knifong, D.L., 2007. Age Determination of the Remaining Peat in the Sacramento-San Joaquin Delta. USGS, California, USA.
- Drexler, J.Z., Fontaine, C.S., Deverel, S.J., 2009. The legacy of wetland drainage on the remaining peat in the Sacramento - San Joaquin Delta, California, USA. *Wetlands* 29, 372–386. <https://doi.org/10.1672/08-97.1>.
- Eichelmann, E., Hemes, K.S., Knox, S.H., Oikawa, P.Y., Chamberlain, S.D., Sturtevant, C., Verfaillie, J.G., Baldocchi, D.D., 2018. The effect of land cover type and structure on evapotranspiration from agricultural and wetland sites in the Sacramento-San Joaquin River Delta, California. *Agric. For. Meteorol.* 256–257. <https://doi.org/10.1016/j.agrformet.2018.03.007>.
- Feldman, D.R., Collins, W.D., Biraud, S.C., Risser, M.D., Turner, D.D., Gero, P.J., Tadić, J., Helmig, D., Xie, S., Mlawer, E.J., Shippert, T.R., Torn, M.S., 2018. Observationally derived rise in methane surface forcing mediated by water vapour trends. *Nat. Geosci.* 11, 238–243. <https://doi.org/10.1038/s41561-018-0085-9>.
- Firestone, M.K., Davidson, E.A., 1989. Microbiological basis of NO and N2O production and consumption in soil. Exchange of Trace Gases Between Terrestrial Ecosystems and the Atmosphere. pp. 7–21.
- Frolking, S., Roulet, N.T., 2007. Holocene radiative forcing impact of northern peatland carbon accumulation and methane emissions. *Glob. Chang. Biol.* <https://doi.org/10.1111/j.1365-2486.2007.01339.x>.
- Goulden, M.L., Litvak, M., Miller, S.D., 2007. Factors that control Typha marsh evapotranspiration. *Aquat. Bot.* 86, 97–106. <https://doi.org/10.1016/j.aquabot.2006.09.005>.
- Griscom, B.W., Adams, J., Ellise, P.W., Houghton, R.A., Lomax, G., 2017. Natural climate solutions. *Proc. Natl. Acad. Sci.* 11–12. <https://doi.org/10.1073/pnas.1710465114>.
- Günther, A., Böther, S., Couwenberg, J., Hüttel, S., Jurasinski, G., 2018. Profitability of Direct Greenhouse Gas Measurements in Carbon Credit Schemes of Peatland Rewetting. <https://doi.org/10.1016/j.ecolecon.2017.12.025>.
- Hanson, B., Putnam, D., Snyder, R., 2007. Deficit irrigation of alfalfa as a strategy for providing water for water-short areas. *Agric. Water Manag.* 93, 73–80. <https://doi.org/10.2495/SI080121>.
- Hatala, J.A., Detto, M., Sonnentag, O., Deverel, S.J., Verfaillie, J.G., Baldocchi, D.D., 2012. Greenhouse gas (CO₂, CH₄, H₂O) fluxes from drained and flooded agricultural peatlands in the Sacramento-San Joaquin Delta. *Agric. Ecosyst. Environ.* 150, 1–18. <https://doi.org/10.1016/j.agee.2012.01.009>.
- Hemes, K.S., Chamberlain, S.D., Eichelmann, E., Knox, S.H., Baldocchi, D.D., 2018a. A biogeochemical compromise: the high methane cost of sequestering carbon in restored wetlands. *Geophys. Res. Lett.* <https://doi.org/10.1029/2018GL077747>.
- Hemes, K.S., Eichelmann, E., Chamberlain, S.D., Knox, S.H., Oikawa, P.Y., Sturtevant, C., Verfaillie, J.G., Szutu, D., Baldocchi, D.D., 2018b. A unique combination of aerodynamic and surface properties contribute to surface cooling in restored wetlands of the Sacramento-San Joaquin Delta, California. *J. Geophys. Res. Biogeosci.* 123, 2072–2090. <https://doi.org/10.1029/2018JG004494>.
- Herbst, M., Friborg, T., Schelde, K., Jensen, R., Ringgaard, R., Vasquez, V., Thomsen, A.G., Soegaard, H., 2013. Climate and site management as driving factors for the atmospheric greenhouse gas exchange of a restored wetland. *Biogeosciences* 10, 39–52. <https://doi.org/10.5194/bg-10-39-2013>.
- Heskel, M.A., Atkin, O.K., Turnbull, M.H., Griffin, K.L., 2013. Bringing the Kok effect to light: a review on the integration of daytime respiration and net ecosystem exchange. *Ecosphere* 4, 1–14. <https://doi.org/10.1890/Es13-00120.1>.
- Hoper, H., Augustin, J., Cagampang, J.P., Drosler, M., Lundin, L., Moors, E., Vasander, H., Waddington, J.M., Wilson, D., 2008. Restoration of peatlands and greenhouse gas balances. In: Strack, M.J. (Ed.), *Peatlands and Climate Change*.
- Kaimal, J.C., Wyngaard, J.C., Izumi, Y., Cot?, O.R., 1972. Spectral characteristics of surface-layer turbulence. *Q. J. R. Meteorol. Soc.* 98, 563–589. <https://doi.org/10.1002/qj.49709841707>.
- Kandel, T.P., Laerke, P.E., Hoffmann, C.C., Elsgaard, L., 2018. Complete annual CO₂, CH₄, and N₂O balance of a temperate riparian wetland 12 years after rewetting. *Ecol. Eng.* <https://doi.org/10.1016/j.ecoleng.2017.12.019>.
- Knox, S.H., Sturtevant, C., Matthes, J.H., Koteen, L., Verfaillie, J.G., Baldocchi, D.D., 2015. Agricultural peatland restoration: effects of land-use change on greenhouse gas (CO₂ and CH₄) fluxes in the Sacramento-San Joaquin Delta. *Glob. Chang. Biol.* 21, 750–765. <https://doi.org/10.1111/gcb.12745>.
- Knox, S.H., Matthes, J.H., Sturtevant, C., Oikawa, P.Y., Verfaillie, J.G., Baldocchi, D.D., 2016. Biophysical controls on interannual variability in ecosystem scale CO₂ and CH₄ exchange in a California rice paddy. *J. Geophys. Res. Biogeosci.* <https://doi.org/10.1002/2015JG003247>. n/a-n/a.
- Knox, S.H., Windham-Myers, L., Anderson, F.E., Sturtevant, C., Bergamaschi, B., 2018. Direct and indirect effects of tides on ecosystem-scale CO₂ exchange in a brackish tidal marsh in Northern California. *J. Geophys. Res. Biogeosci.* <https://doi.org/10.1002/2017JG004048>.
- Krauss, K.W., Holm, G.O., Perez, B.C., McWhorter, D.E., Cormier, N., Moss, R.F., Johnson, D.J., Neubauer, S.C., Raynie, R.C., 2016. Component greenhouse gas fluxes and radiative balance from two deltaic marshes in Louisiana: pairing chamber techniques and eddy covariance. *J. Geophys. Res. Biogeosci.* 121, 1503–1521. <https://doi.org/10.1002/2015JG003224>.
- Krauss, K.W., Noe, G.B., Duberstein, J.A., Conner, W.H., Stagg, C.L., Cormier, N., Jones, M.C., Bernhardt, C.E., Graeme Lockaby, B., From, A.S., Doyle, T.W., Day, R.H., Ensign, S.H., Pierfelice, K.N., Hupp, C.R., Chow, A.T., Whitbeck, J.L., 2018. The role of the upper tidal estuary in wetland blue carbon storage and flux. *Global Biogeochem. Cycles* 32, 817–839. <https://doi.org/10.1029/2018GB005897>.
- Lee, S.C., Christen, A., Black, A.T., Johnson, M.S., Jassal, R.S., Ketler, R., Nesic, Z., Merken, M., 2016. Annual greenhouse gas budget for a bog ecosystem undergoing restoration by rewetting. *Biogeosci. Discuss.* 1, 1–26. <https://doi.org/10.5194/bg-2016-446>.
- Leifeld, J., Menichetti, L., 2018. The underappreciated potential of peatlands in global climate change mitigation strategies. *Nat. Commun.* 9, 1071. <https://doi.org/10.1038/s41467-018-03406-6>.
- McNicol, G., Sturtevant, C.S., Knox, S.H., Dronova, I., Baldocchi, D.D., Silver, W.L., 2016. Effects of seasonality, transport-pathway, and spatial structure on greenhouse gas fluxes in a restored wetland. *Glob. Chang. Biol.* 1–15. <https://doi.org/10.1111/gcb.13580>.
- Miller, R.L., Fram, M., Fujii, R., Wheeler, G., 2008. Subsidence reversal in a Re-established wetland in the Sacramento-San Joaquin Delta, California, USA. *San Fr. Estuary Watershed Sci.* 6.
- Mitsch, W.J., Mander, Ü., 2018. Wetlands and carbon revisited. *Ecol. Eng.* 114, 1–6. <https://doi.org/10.1016/j.ecoleng.2017.12.027>.
- Moffat, A.M., Papale, D., Reichstein, M., Hollinger, D.Y., Richardson, A.D., Barr, A.G., Beckstein, C., Braswell, B.H., Churkina, G., Desai, A.R., Falge, E., Gove, J.H., Heimann, M., Hui, D., Jarvis, A.J., Kattge, J., Noormets, A., Stauch, V.J., 2007. Comprehensive comparison of gap-filling techniques for eddy covariance net carbon fluxes. *Agric. For. Meteorol.* 147, 209–232. <https://doi.org/10.1016/j.agrformet.2007.08.011>.
- Moreno-Mateos, D., Power, M.E., Comín, F.A., Yockteng, R., 2012. Structural and functional loss in restored wetland ecosystems. *PLoS Biol.* 10. <https://doi.org/10.1371/journal.pbio.1001247>.
- Moreno-Mateos, D., Barbier, E.B., Jones, P.C., Jones, H.P., Aronson, J., López-López, J.A., McCrackin, M.L., Meli, P., Montoya, D., Rey Benayas, J.M., 2017. Anthropogenic ecosystem disturbance and the recovery debt. *Nat. Commun.* 8, 8–13. <https://doi.org/10.1038/ncomms14163>.
- Myhre, G., Shindell, D., Bréon, F.-M., Collins, W., Fuglestad, J., Huang, J., Koch, D.,

- Lamarque, J.-F., Lee, D., Mendoza, B., Nakajima, T., Robock, A., Stephens, G., Takemura, T., Zhang, H., 2013. 2013: anthropogenic and natural radiative forcing. *Climate Change 2013: The Physical Science Basis. Contribution of Working Group I to the Fifth Assessment Report of the Intergovernmental Panel on Climate Change*.
- Neubauer, S.C., Magonigal, J.P., 2015. Moving beyond global warming potentials to quantify the climatic role of ecosystems. *Ecosystems*. <https://doi.org/10.1007/s10021-015-9879-4>.
- Nisbet, E.G., Dlugokencky, E.J., Manning, M.R., Lowry, D., Fisher, R.E., France, J.L., Michel, S.E., Miller, B., White, J.W.C., Vaughn, B., Bousquet, P., Pyle, J.A., Warwick, N.J., Cain, M., Brownlow, R., Zazzeri, G., Lanoisell, M., Manning, A.C., Gloor, E., Worthy, D.E.J., Brunke, E.-G., Labuschagne, C., Wolff, E.W., Ganesan, A.L., 2016. Rising atmospheric methane: 2007–2014 growth and isotopic shift. *Glob. Biogeochem. Cycles* 30, 1–15. <https://doi.org/10.1002/2015GB005326>. Received.
- Odum, E., 1969. The strategy of ecosystem development. *Science* (80-) 164, 262–270.
- Oikawa, P.Y., Jenerette, G.D., Knox, S.H., Sturtevant, C., Verfaillie, J.G., Dronova, I., Poindexter, C.M., Eichelmann, E., Baldocchi, D.D., 2016a. Evaluation of a hierarchy of models reveals importance of substrate limitation for predicting carbon dioxide and methane exchange in restored wetlands. *J. Geophys. Res. Biogeosci.* <https://doi.org/10.1002/2016JG003438>.
- Oikawa, P.Y., Sturtevant, C., Knox, S.H., Verfaillie, J.G., Huang, Y., Baldocchi, D.D., 2016b. Revisiting the partitioning of net ecosystem exchange of CO₂ into photosynthesis and respiration with simultaneous flux measurements of 13CO₂ and CO₂, soil respiration and a biophysical model, CANVEG. *Agric. For. Meteorol.* 234–235. <https://doi.org/10.1016/j.agrformet.2016.12.016>. in press.
- Papale, D., Reichstein, M., Aubinet, M., Canfora, E., Bernhofer, C., Kutsch, W., Longdoz, B., Rambal, S., Valentini, R., Vesala, T., Yakir, D., 2006. Towards a standardized processing of Net Ecosystem Exchange measured with eddy covariance technique: algorithms and uncertainty estimation. *Biogeosciences* 3, 571–583. <https://doi.org/10.5194/bg-3-571-2006>.
- Pathak, T., Maskey, M., Dahlberg, J., Kearns, F., Bali, K., Zaccaria, D., 2018. Climate change trends and impacts on California agriculture: a detailed review. *Agronomy* 8, 25. <https://doi.org/10.3390/agronomy8030025>.
- Paustian, K., Lehmann, J., Ogle, S., Reay, D., Robertson, G.P., Smith, P., 2016. Climate-smart soils. *Nature* 532, 49–57. <https://doi.org/10.1038/nature17174>.
- Perugini, L., Caporaso, L., Marconi, S., Cescatti, A., Quesada, B., de Noblet, N., House, J., Arneth, A., 2017. Biophysical effects on temperature and precipitation due to land cover change. *Environ. Res. Lett.* <https://doi.org/10.1088/1748-9326/aa6b3f>.
- Petrescu, A.M.R., Lohila, A., Tuovinen, J.-P., Baldocchi, D.D., Desai, A.R., Roulet, N.T., Vesala, T., Dolman, A.J., Oechel, W.C., Marcolla, B., Friborg, T., Rinne, J., Matthes, J.H., Merbold, L., Meijide, A., Kiely, G., Sottocornola, M., Sachs, T., Zona, D., Varlagin, A., Lai, D.Y.F., Veenendaal, E., Parmentier, F.-J.W., Skiba, U., Lund, M., Hensen, A., van Huissteden, J., Flanagan, L.B., Shurpali, N.J., Grünwald, T., Humphreys, E.R., Jackowicz-Korczyński, M., Aurela, M.A., Laurila, T., Grünig, C., Corradi, C.A.R., Schrier-Uijl, A.P., Christensen, T.R., Tamstorf, M.P., Mastepanov, M., Martikainen, P.J., Verma, S.B., Bernhofer, C., Cescatti, A., 2015. The uncertain climate footprint of wetlands under human pressure. *Proc. Natl. Acad. Sci. U. S. A.* 112, 4594–4599. <https://doi.org/10.1073/pnas.1416267112>.
- Poulter, B., et al., 2017. Global wetland contribution to 2000–2012 atmospheric methane growth rate dynamics. *Environ. Res. Lett.* 12. <https://doi.org/10.1088/1748-9326/aa8391>.
- Psarras, P., Krutka, H., Fajardy, M., Zhang, Z., Liguori, S., Dowell, N.Mac, Wilcox, J., 2017. Slicing the pie: how big could carbon dioxide removal be? *Wiley Interdiscip. Rev. Energy Environ.* 6, e253. <https://doi.org/10.1002/wene.253>.
- Richardson, A.D., Hollinger, D.Y., 2007. A method to estimate the additional uncertainty in gap-filled NEE resulting from long gaps in the CO₂ flux record. *Agric. For. Meteorol.* 147, 199–208. <https://doi.org/10.1016/j.agrformet.2007.06.004>.
- Roulet, N.T., 2000. Peatlands, carbon storage, greenhouse gases, and the Kyoto Protocol: prospects and significance for Canada. *Wetlands* 20, 605–615. [https://doi.org/10.1672/0277-5212\(2000\)020\[0605:PCSGGA\]2.0.CO;2](https://doi.org/10.1672/0277-5212(2000)020[0605:PCSGGA]2.0.CO;2).
- Roulet, N.T., Lafleur, P.M., Richard, P.J.H., Moore, T.R., Humphreys, E.R., Bubier, J., 2007. Contemporary carbon balance and late Holocene carbon accumulation in a northern peatland. *Glob. Chang. Biol.* <https://doi.org/10.1111/j.1365-2486.2006.01292.x>.
- Sanderman, J., Hengl, T., Fiske, G.J., 2017. Soil carbon debt of 12,000 years of human land use. *Proc. Natl. Acad. Sci.* 201706103. <https://doi.org/10.1073/PNAS.1706103114>.
- Schrier-Uijl, A.P., Kroon, P.S., Hendriks, D.M.D., Hensen, A., Van Huissteden, J., Berendse, F., Veenendaal, E.M., 2014. Agricultural peatlands: towards a greenhouse gas sink - a synthesis of a Dutch landscape study. *Biogeosciences*. <https://doi.org/10.5194/bg-11-4559-2014>.
- Sturtevant, C., Ruddell, B.L., Knox, S.H., Verfaillie, J.G., Matthes, J.H., Oikawa, P.Y., Baldocchi, D.D., 2016. Identifying scale-emergent, nonlinear, asynchronous processes of wetland methane exchange. *J. Geophys. Res. Biogeosciences* 121, 188–204. <https://doi.org/10.1002/2015JG003054>.
- Syvitski, J.P.M., Kettner, A.J., Overeem, I., Hutton, E.W.H., Hannon, M.T., Brakenridge, G.R., Day, J., Vörösmarty, C., Saito, Y., Giosan, L., Nicholls, R.J., 2009. Sinking deltas due to human activities. *Nat. Geosci.* 2, 681–686. <https://doi.org/10.1038/ngeo629>.
- Teh, Y.A., Silver, W.L., Sonnentag, O., Detto, M., Kelly, M., Baldocchi, D.D., 2011. Large greenhouse gas emissions from a temperate peatland pasture. *Ecosystems* 14, 311–325. <https://doi.org/10.1007/s10021-011-9411-4>.
- Tiedje, J.M., 1988. Ecology of denitrification and dissimilatory nitrate reduction to ammonium. *Biology of Anaerobic Microorganisms*. Wiley-Interscience Publication, Canada, pp. 179–244.
- Veber, G., Kull, A., Villa, J.A., Maddison, M., Paal, J., Oja, T., Iturraspe, R., Pärn, J., Teemusk, A., Mander, Ü., 2017. Greenhouse gas emissions in natural and managed peatlands of America: case studies along a latitudinal gradient. *Ecol. Eng.* <https://doi.org/10.1016/j.ecoleng.2017.06.068>.
- Webb, E.K., Pearman, G.I., Leuning, R., 1980. Correction of flux measurements for density effects due to heat and water vapour transfer. *Q. J. R. Meteorol. Soc.* 106, 85–100. <https://doi.org/10.1002/qj.49710644707>.
- Weir, W.W., 1950. Subsidence of peatlands of the Sacramento-San Joaquin Delta, California. *Hilgardia* 20.
- Wilson, D., Blain, D., Couwenberg, J., Evans, C.D., Murdiyasar, D., Page, S.E., Renou-Wilson, F., Rieley, J.O., Sirin, A., Strack, M., Tuittila, E.-S., 2016a. Greenhouse gas emission factors associated with rewetting of organic soils. *Mires Peat* 17, 1–28. <https://doi.org/10.19189/Map.2016.OMB.222>.
- Wilson, D., Farrell, C.A., Fallon, D., Moser, G., Müller, C., Renou-Wilson, F., 2016b. Multi-year greenhouse gas balances at a rewetted temperate peatland. *Glob. Chang. Biol.* <https://doi.org/10.1111/gcb.13325>.
- Windham-Myers, L., Bergamaschi, B., Anderson, F., Knox, S., Miller, R., Fujii, R., 2018. Potential for negative emissions of greenhouse gases (CO₂, CH₄ and N₂O) through coastal peatland re-establishment: novel insights from high frequency flux data at meter and kilometer scales. *Environ. Res. Lett.* 13. <https://doi.org/10.1088/1748-9326/aaae74>.
- Yarwood, S.A., 2018. The role of wetland microorganisms in plant-litter decomposition and soil organic matter formation: a critical review. *FEMS Microbiol. Ecol.* 1–17. <https://doi.org/10.1093/femsec/fiy175>.
- Zhang, B., Tian, H., Lu, C., Chen, G., Pan, S., Anderson, C., Poulter, B., 2017. Methane emissions from global wetlands: an assessment of the uncertainty associated with various wetland extent data sets. *Atmos. Environ.* 165, 310–321. <https://doi.org/10.1016/j.atmosenv.2017.07.001>.